Computed electron oscillation inside the duct of a vacuum arc source

T. K. Kwok, T. Zhang, and P. K. Chu[a)]
Department of Physics and Materials Science, City University of Hong Kong, 83 Tat Chee Avenue, Kowloon, Hong Kong

M. M. M. Bilek
Department of Engineering, University of Cambridge, Cambridge CB2 1PZ, United Kingdom

I. G. Brown
Lawrence Berkeley National Laboratory, University of California, Berkeley, California 94720

(Received 17 November 1998; accepted for publication 1 February 1999)

A three-dimensional numerical model has been developed to simulate the motion of electrons inside the duct of a vacuum arc metal source. It is found that electrons will travel back and forth along the center axis inside the duct tube. This phenomenon of electron oscillation can be explained by the combined effects of the electric and magnetic fields. The electron oscillation will increase the charge state of the positive ions and the ions will gain more energy. Due to the influence of electron oscillation, the plasma throughput of the duct will be different from that of a duct under the influence of only the magnetic field. This finding should be taken into account when designing metal arc sources and optimizing their performance. © *1999 American Institute of Physics.* [S0021-8979(99)05209-3]

I. INTRODUCTION

Vacuum arc or cathodic arc metal sources can deposit high quality thin metal films and metallurgical coatings.[1–3] A metal plasma consisting of positive metal ions and electrons is created when an arc discharge is triggered between two metal electrodes in vacuum. Metal plasma immersion ion implantation and deposition (MEPIIID), a hybrid process combining cathodic arc deposition and plasma immersion ion implantation, is a novel surface modification technology.[4] This technique which encompasses coimplantation of gaseous and metallic ions can improve the wear and corrosion resistance of the treated surface.

The plasma generated by the metal vacuum arc comprises electrons, ions with charge states between $1+$ to $5+$, a small fraction of neutral atoms ($<1\%$), and macroparticles typically micrometers in size.[5] Contamination of the thin metal films by macroparticles is the major disadvantage precluding a wide application of vacuum arc plasma sources in the industry. The macroparticle velocity is in the range of 100 m/s, and the plasma velocity is typically much higher at 1 to 2×10^4 m/s.[6,7] Consequently, they can be removed by a magnetic field using either a straight[8,9] or curved[4,5,8,10–13] geometry. The magnetic field can guide the metal plasma from the source to the target while the macroparticles cannot reach the target because they collide with the duct walls due to their inertia. One drawback of the magnetic duct is the reduction of the plasma flux on account of recombination at the duct walls. In order to increase the throughput of the metal plasma, the curved magnetic duct wall can be biased with a positive voltage.[14] Alternatively, a quarter of the duct wall area can be positively biased at its outer major circumference by inserting a curved plate electrode such as a Bilek biased plate.[15] The maximum transport occurs at a biased voltage of about $+20$ V.[5,10,12] The combination of magnetic and electric field can give rise to an increase in the plasma transport efficiency on the order of 25%.[5]

In previous works, the electron motion in a vacuum arc has not been probed but it is an important factor. The electron density is usually two or three times that of the ion density.[16] The magnetic field generated by the duct is usually around a few tens of milli-tesla.[10,14,15] The field strength is strong enough to magnetize the electrons but not the ions. The magnetized electrons will follow the magnetic field line. Due to the internal electric field in the plasma, the ion motion will be coupled to that of the electrons, and the plasma will rotate along the central axis of the duct (model of ''plasma optics'').[4,10]

In this article, we will present our simulation results on the electron trajectories inside the duct of the vacuum arc source. Different working conditions will be investigated. Our results show that under the combined effects of the electric and magnetic fields, the electrons will oscillate along the center axis inside the duct tube [Fig. 1(a)] and drift to the $-z$ direction (Fig. 2) of the duct tube. This phenomenon and its effects will be discussed. Electron oscillation will increase the probability of collision with ions and increase the charged state of the positive ions. This phenomenon should thus be taken into account in metal arc source design and its optimization.

II. SIMULATION MODEL AND FORMALISM

We use a three-dimensional model to simulate the electron trajectory along the duct filter using cylindrical coordinates (ρ, ϕ, z) as illustrated in Fig. 1. The symmetry axis of the curved duct is rested in the $z=0$ plane of Fig. 2. The center of the major curvature is placed at the origin. As

a)Corresponding author; Electronic mail: paul.chu@cityu.edu.hk

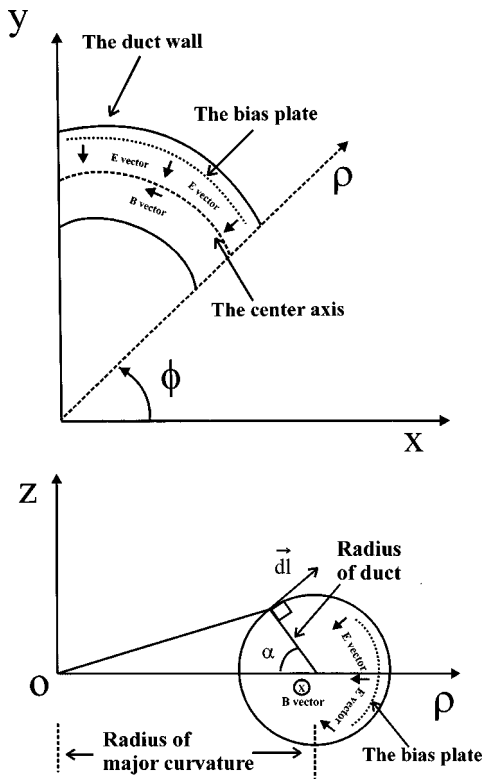

FIG. 1. Schematic of the curved duct in cylindrical coordinates along (a) the $(\rho,\ \phi)$ plane, and (b) the (ρ,z) plane. The bias plate, **E** field, and **B** field vectors are indicated.

shown in Fig. 1, the length of the duct is related to ϕ. The magnetic field is generated by the coils surrounding the duct. The field $d\mathbf{B}$ at a point due to an element of the duct coil is represented by:

$$d\mathbf{B}=\frac{\mu_0 In(\rho d\phi)d\mathbf{l}\mathbf{r}}{4\pi r^3}, \tag{1}$$

where μ_0 is the permeability, I is the current in the duct coils, n is number of turns per unit length, $\rho d\phi$ is the length of the element along ϕ, **r** is a vector between the point and the element, and $d\mathbf{l}$ is a vector tangent to the surface of the duct as depicted in Fig. 1:

$$d\mathbf{l}=R_{\mathrm{minor}}d\alpha(\cos\alpha\hat{k}+\sin\alpha\hat{\rho}) \tag{2}$$

The ultimate magnetic field at a point in space can be calculated by integrating Eq. (1) for all the duct coils.

The electric field is generated by the positive voltage applied to the bias plate placed at the outer wall of the curved duct. The potential Φ in space can be expressed by Poisson's equation

$$\nabla^2\Phi=-\frac{(\Sigma q_i n_i-qn_e)}{\epsilon_0}, \tag{3}$$

where q is the elementary charge, q_i is constituent charge, ϵ_0 is the dielectric constant, and n_i and n_e are the ion and electron density, respectively. In our work, the main concern is the motion of the electrons and n_i and n_e are assumed to be zero. In cylindrical coordinates, it becomes

$$\frac{1}{\rho}\frac{\partial}{\partial\rho}\left(\rho\frac{\partial\Phi}{\partial\rho}\right)+\frac{1}{\rho^2}\frac{\partial^2\Phi}{\partial\phi^2}+\frac{\partial^2\Phi}{\partial z^2}=0. \tag{4}$$

Equation (4) can be solved by the finite difference method. A rectangular mesh is applied to the (ρ,z) plane [Fig. 1(b)]. The circular boundary of the duct wall will not lie on the grid line. We simply adopt the ''irregular physical boundaries'' method to express the first and second order derivatives in terms of the value at the boundary rather than at the node.[17] The potential of each grid point is obtained by iteration. The trajectory of a charged particle under the influence of electric **E** and magnetic **B** fields can be described by the kinematic equations

$$m\frac{d\mathbf{V}}{dt}=q(\mathbf{E}+\mathbf{V}\times\mathbf{B}), \tag{5}$$

$$\frac{d\mathbf{r}_p}{dt}=\mathbf{V}, \tag{6}$$

where q is the charge of the particle, **V** is the velocity, and $\mathbf{r}_p$ is the position of the particle. **E** and **B** are position dependent. Usually, the electrons are well confined by the magnetic field. Equations (5) and (6) are simplified by incorporating the **E**×**B** drifts of the electron. We will ignore the gyrating motion of the electrons and only consider their average motion. The velocity and electric field are resolved into two components, one parallel to the magnetic field and the other perpendicular to the magnetic field. Equation (5) becomes

$$m\frac{d(\mathbf{V}_{\|B}+\mathbf{V}_{\perp B})}{dt}=q(\mathbf{E}_{\|B}+\mathbf{E}_{\perp B}+\mathbf{V}_{\|B}\times\mathbf{B}+\mathbf{V}_{\perp B}\times\mathbf{B}). \tag{7}$$

$\mathbf{V}_{\|B}\times\mathbf{B}=0$ and Eq. (7) can be separated into two equations:

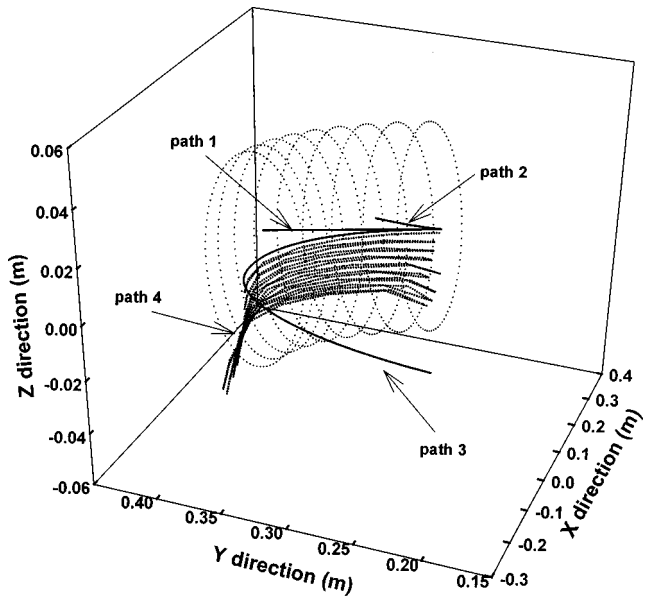

FIG. 2. Four electron trajectories under different conditions. Path 1 is the trajectory without applying either the electric or magnetic field. Path 2 is the trajectory with only the electric field. Path 3 is the trajectory with only the magnetic field. Path 4 is the trajectory under the influence of both the electric and magnetic field, and the electron oscillates along the axis of the curved duct.

$$m\frac{d\mathbf{V}_{\|B}}{dt}=q\mathbf{E}_{\|B}, \tag{8a}$$

$$m\frac{d\mathbf{V}_{\perp B}}{dt}=q(\mathbf{E}_{\perp B}+\mathbf{V}_{\perp B}\times\mathbf{B}). \tag{8b}$$

The solution of Eq. (8b) is $\mathbf{V}_{\perp B}=\mathbf{V}_D+\mathbf{V}_{gy}$, where $\mathbf{V}_D$ is the drift velocity, i.e.,

$$\mathbf{V}_D=\frac{\mathbf{E}_{\perp B}\times\mathbf{B}}{|B|^2} \tag{9}$$

and $\mathbf{V}_{gy}$ is the gyration velocity of the electron which is ignored in our simulation. By solving Eq. (8a), the final velocity of the electron becomes $\mathbf{V}=\mathbf{V}_{\|B}+\mathbf{V}_D$. The position of the electron is numerically updated by Eq. (6.) The iterative process is repeated at the updated position until the end of the simulation.

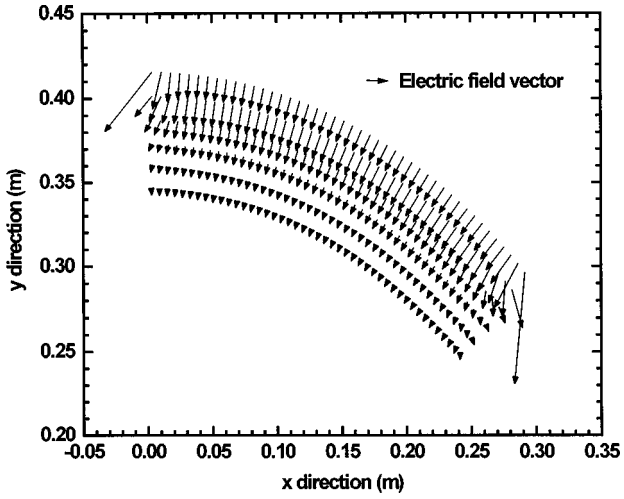

FIG. 3. Electric field vector along the symmetry plane of the curved duct ($z=0$).

III. RESULTS AND DISCUSSION

The electron motion of a single particle inside the duct is modeled based on the dimensions of the instrument at the City University of Hong Kong.[18] The duct in the cathodic vacuum arc source has a 45° filter tube. The major radius of curvature at its axis is 38 cm and the internal radius of the duct is 4 cm. The curved Bilek biased plate is placed at the outer circumference covering a quarter of the inner surface of the duct. The number of turns of the duct coil is 10 350. When applying a coil current of 6 A, the maximum magnetic field at the center of the duct coils in the middle of the duct tube is 240 Gauss. Five volts are applied to the biased plate. An electron is normally fired at one end of the duct position at the center with an initial velocity of 1.5×10^4 m/s. Figure 2 displays the trajectories of the electron in the absence of plasma effects under four conditions and the duct wall is represented by the dotted circles.

Path 1 in Fig. 2 represents the electron trajectory without the electric and magnetic fields. The electron goes straight and is stopped by the outer duct wall at 1.181×10^{-5} s. The electron travels a total distance of 0.1772 m. This simple calculation verifies our model is simulating properly the motion of an electron in cylindrical coordinates.

Path 2 in Fig. 2 depicts the electron trajectory under the attraction of an electric field produced by applying 5 V to the biased plate. It took only 9.048×10^{-8} s for the electron to be absorbed by the outer duct wall. The electric field created by the biased plate will repel most of the positive ions but will not provide a central stream of electrons when working on its own. Therefore, the ''model of plasma optics'' cannot be applied in this situation.

Path 3 in Fig. 2 shows the electron trajectory under the influence of a magnetic field. The electron is well confined and travels through the duct following the magnetic field lines. The electron stays in the duct for about 2×10^{-5} s and takes 4×10^{-5} s to arrive at the final position illustrated in Fig. 2. The initial position of the electron is assumed to have a Gaussian distribution at the opening end of the duct plane. According to the model of plasma optics, a central beam of electrons will pass through the duct tube but expand widely when exiting the duct since the magnetic field lines are no longer concentrated at the center axis outside the duct. Under the influence of the electrons, the positive ions will expand forming a wide and uneven distribution in concentration when exiting the duct tube. The degree of widening obviously depends on the distance away from the duct exit.

Path 4 is the most complicated one. It shows the trajectory of an electron under the combined influence of both the electric and magnetic fields. The electron is found to traverse back and forth inside the duct tube along the center axis. As the electron oscillates, it drifts to the $-z$ direction of the duct until it hits the duct wall. The electron stays in the duct tube for 1.181×10^{-5} s. The electron oscillation phenomenon can be explained as follows. Figure 3 is a vector plot of the electric field along the symmetry plane of the center axis of the duct tube at $z=0$. It shows that the electric field inside the duct tube is perpendicular to the curved duct. In other words, the electric field is perpendicular to the magnetic field lines. Therefore, when the electron traverses inside the duct, instead of getting attracted by the electric field towards the outer duct wall (path 2 in Fig. 2), it will drift due to the $E\times B$ force. From the right hand rule, the $E\times B$ force will force the electron downward in the $-z$ direction. The electric field vectors at the start and at the end of the duct tube are different. They expand radically outwards and are stronger than those inside the tube. The electric field vectors of the entrance and exit of the tube are not mirror images as a grounded mask is usually inserted at the entrance of the duct.[16] The radial component of the electric field at both ends will decelerate the electron and attract it back into the duct forming a ''simple harmonic field trap.''

We do not believe that all the electrons inside the duct will oscillate because it depends on the initial position of each electron and the effects of the plasma have to be considered as well. In the presence of the plasma, the internal plasma field will drive the electrons. Moreover, the electrons will couple with the positive ions and scatter with other electrons. Nonetheless, even if some of the electrons are oscillating, they will produce a pronounced effect on the plasma

motion. The oscillating electrons will increase the chance of scattering and collision with the ions. Hence, the charge state of the ions will increase and the ions will gain more energy. The $E \times B$ force will drift the electrons downward in the -z direction. The electron beam will not lie along the central axis and the plasma may rotate towards the bottom of the duct tube. Some of the electrons will simply not leave the duct tube. The distribution of the ions will be quite different from that with the magnetic field alone. The ions will be more concentrated when leaving the duct.

One of the purposes of inserting a biased plate covering a quarter of the outer duct wall instead of biasing the whole duct is to reduce the electrons lost to the duct wall.[15] However, we have shown that the combined effect of the electric and magnetic field is providing a $E \times B$ force drifting the electrons. Thus, the degree of flux enhancement by biasing the whole duct wall must be reconsidered.[15]

IV. CONCLUSION

In summary, we have employed a three dimensional model to simulate the electron motion inside a vacuum arc metal plasma duct. The model predicts the electron trajectory with and without the electric and/or magnetic field. Under the combined effects of the electric and magnetic field, the electrons are found to oscillate inside the duct tube. This phenomenon arises from the $E \times B$ force and is a new concept for vacuum arc metal plasma sources. The charge state of the positive ions will be increased and the plasma motion will be altered. The new phenomenon should be taken into account in the design of metal arc sources.

ACKNOWLEDGMENTS

This work was supported by Hong Kong RGC Earmarked Grant Nos. 9040332 and 9040344.

[1] R. L. Boxman, S. Goldsmith, S. Shalev, H. Yaloz, and N. Brosh, Thin Solid Films **139**, 41 (1986).
[2] R. L. Boxman and S. Goldsmith, IEEE Trans. Plasma Sci. **17**, 705 (1989).
[3] S. Anders, A. Anders, and I. Brown, J. Appl. Phys. **74**, 4239 (1993).
[4] A. Anders, Surf. Coat. Technol. **93**, 158 (1997).
[5] A. Anders, S. Anders, and I. G. Brown, Plasma Sources Sci. Technol. **4**, 1 (1995).
[6] J. Kutzner and H. C. Miller, J. Phys. D **25**, 686 (1992).
[7] B. Gellert and E. Schade, *Proceedings of the XIVth International Symposium on Discharges and Electrical Insulation in Vacuum*, 1990, Santa Fe (IEEE, New York, 1990), p. 450.
[8] J. Storer, J. E. Galvin, and I. G. Brown, J. Appl. Phys. **66**, 5245 (1989).
[9] I. I. Aksenov, V. G. Padalka, V. T. Tolok, and V. M. Khoroshikh, Fiz. Plazmy **6**, 918 (1980); Sov. J. Plasma Phys. **6**, 504 (1980).
[10] A. Anders, S. Anders, and I. G. Brown, J. Appl. Phys. **75**, 4900 (1994).
[11] S. Falabella and D. M. Sanders, J. Vac. Sci. Technol. A **10**, 394 (1992).
[12] I. I. Aksenov, V. A. Belous, V. G. Padalka, and V. M. Khoroshikh, Fiz. Plazmy **4**, 758 (1978); Sov. J. Plasma Phys. **4**, 425 (1978).
[13] I. I. Aksenov, V. A. Belous, V. G. Padalka, and V. M. Khoroshikh, Prib. Tekh. Eksp. **5**, 236 (1978); Instrum. Exp. Tech. **21**, 1416 (1978).
[14] M. M. M. Bilek, Y. B. Yin, and D. R. McKenzie, IEEE Trans. Plasma Sci. **24**, 1165 (1996).
[15] M. M. M. Bilek, D. R. McKenzie, Y. B. Yin, M. U. Chhowalla, and W. I. Milne, IEEE Trans. Plasma Sci. **24**, 1291 (1996).
[16] A. Anders, Phys. Rev. E **55**, 969 (1997).
[17] Paul L. DeVries, *A First Course in Computational Physics* (Wiley, New York, 1994).
[18] P. K. Chu, S. Qin, C. Chan, N. W. Cheung, and L. A. Larson, Mater. Sci. Eng., R. **R17(6-7)**, 207 (1996).